Research on underwater acoustic channel estimation and temperature factors based on FBMC

GUO Yin-jing[1,2], LIU Zhen[1], YANG Wen-jian[1], NIU Chen-xi[1], LIU Hui[1]

(1. *College of Electronic Information Engineering, Shandong University of Science and Technology, Qingdao 266590, China*; 2. *Qingdao Zhihai Muyang Technology Co., Ltd., Qingdao 266590, China*)

Abstract: The complexity of underwater environment poses a challenge to underwater acoustic communication. In marine environment, different temperatures, depths and salinities would affect the performance of acoustic communication. The analysis of the underwater acoustic channel under the influence of temperature factors provides a reference for further study of the underwater acoustic channel estimation problem based on filter bank multi-carrier (FBMC). The FBMC based offset quadrature amplitude modulation (OQAM) technology (FBMC/OQAM) was introduced into the underwater acoustic communication. Based on FBMC, the underwater acoustic channel estimation technology was studied. By changing the pilot structure to adapt to the complex and variable underwater acoustic channel, the iterative method was used to obtain the channel information with higher accuracy and further improve the performance of channel estimation. Theoretical analysis and simulation results show that iterative channel estimation algorithm based on the new interference approximation method (IAM) pilot proposed in this paper has better performance in underwater acoustic channel.

Key words: filter bank multi-carrier (FBMC); underwater acoustic channel estimation; temperature; pilot; interference approximation method (IAM)

CLD number: TJ630.33; U675.7; U674.941 **doi**: 10.3969/j.issn.1674-8042.2020.02.013

0 Introduction

Ocean area accounts for 71% of the Earth's total area, and marine resources are of great significance to human development. At present, because orthogonal frequency division multiplexing (OFDM) based on cyclic prefix (CP-OFDM) has features such as robustness to multipath effects and high spectral efficiency, it is adopted in underwater acoustic communication. Inter-symbol interference (ISI) and inter-carrier interference (ICI) caused by cyclic prefix in OFDM will affect the communication system. The fifth generation cellular radio (5G) proposes to apply filter bank multi-carrier (FBMC) technology to wireless communication system[1-2]. The prototype filters of the FBMC/offset quadrature amplitude modulation (OQAM) system include a raised cosine filter, a PHYDYAS filter[3], an isotropic orthogonal transform algorithm (IOTA) filter[4] and so on. Because such prototype filters could reduce side lobes, FBMC/OQAM can alleviate ISI and ICI issues to provide higher transmission rates without guard intervals or cyclic prefixes unlike OFDM. Studies have shown that the application of FBMC/OQAM modulation scheme can outperform CP-OFDM in terms of bit error rate (BER) and spectral efficiency[5]. The influence of underwater acoustic communication technology on underwater positioning and navigation is also irreplaceable. It is a hot research topic to optimize the channel estimation technology to achieve high speed and reliability of underwater communication.

Like other communication systems, channel estimation is critical for the FBMC/OQAM system to recover transmitted data at the receiver. Since the FBMC system only satisfies the real number field orthogonality, many channel estimation methods available for OFDM systems cannot be directly applied to the FBMC/OQAM system. This means that in FBMC/OQAM transmission, real-valued data will be subject to inherent interference from imaginary-valued data[6]. Aiming at the interference

Received date: 2019-09-08

Foundation items: Focus on Research and Development Plan in Shandong Province (Special Public Welfare Project) (No. 2018GHY115022); National Natural Science Foundation of China (No. 61471224)

Corresponding author: LIU Zhen (1205762091@qq.com)

of imaginary part, researches have proposed some channel estimation methods based on FBMC system. According to different interference mechanisms, these pilot-assisted channel estimation methods can be divided into three categories: the first method is based on interference cancellation. The pilot structure is designed at the transmitter, so that the inherent interference does not affect the pilot position, and the conventional channel estimation method can be directly used at the receiver, such as auxiliary pilot (AP)[7], code auxiliary pilot method (CAP)[8] and discrete fourier transformation (DFT)-based FBMC system channel estimation method[9]. The interference cancellation method achieves better channel tracking performance while reducing spectral efficiency or increasing computational complexity[6]. The second method is based on the interference approximation method (IAM), for example, IAM-real (IAM-R)[10] whose pilot value is a real value of ± 1, so that the interference of the pilot symbols from the first-order neighbors contributes to channel estimation. IAM-imaginary (IAM-I) is similar to IAM-R, with an intermediate pilot element of $\pm$j. IAM-complex (IAM-C) is an improved method of IAM-R with an intermediate pilot element of ± 1 or $\pm$j[11]. To further improve performance, an extended version of IAM-C (called as EIAM-C) is proposed, with two pilot values around the pilot sequence being ± 1 or $\pm$j[12]. The IAM can maximize the effect of intrinsic interference on the channel and realize channel estimation of the FBMC/OQAM system. The third method is the channel estimation method based on interference avoidance. The channel frequency domain response is derived mainly by computational techniques or filtering, such as paired pilot method (POP). The advantage is that the whole system is not inherently designed. The interference calculation cancels out the inherent interference of the system in terms of operation. The disadvantage is that the POP scheme needs to be determined by the inverse equalizer, which leads to further errors, such as noise enhancement[13].

In a complex marine environment, the speed of sound in water depends on the depth, temperature and salinity of the seawater[14]. Based on the FBMC/OQAM system, this paper conducts a comprehensive study on underwater temperature factors and underwater acoustic channel estimation techniques. On the basis of IAM, the IAM pilot is improved. The channel estimation accuracy is improved by multiple iterations, and its performance is verified by simulation.

1 FBMC system model

1.1 Bastic theory of FBMC/OQAM system

The modulation and demodulation block diagram of the FBMC/OQAM system is shown in Fig. 1, where M indicates the number of subcarriers, $a_{m,n}$ represents the n-th OQAM symbol of the m-th carrier, and $m \in \{1, 2, \cdots, M-1\}$. The steps of obtaining OQAM data are as follows: firstly, the transmission bit stream pass through the quadrature amplitude modulation (QAM) to obtain a complex symbol; secondly, the real number symbols are obtained by the real part and the imaginary part of the complex symbol; lastly, these data are transmitted by the virtual real part misalignment half symbol period. $g(k)$ is a real symmetric prototype filter with length of L. The data symbol $a_{m,n}$ is firstly multiplied the phase factor $e^{j\pi(m+n)/2}$ to keep the real field orthogonal between the subcarrier and the FBMC symbol. Then, all data is modulated by inverse fast fourier transform (IFFT) onto the subcarriers, and added together after passing the prototype filter outputs. Lastly, transmit over the channel. Similarly, in order to recover the transmitted data, the received data is demodulated by a filter combined Fourier transform, and the signal on the subcarrier is converted into a complex signal by OQAM post processing.

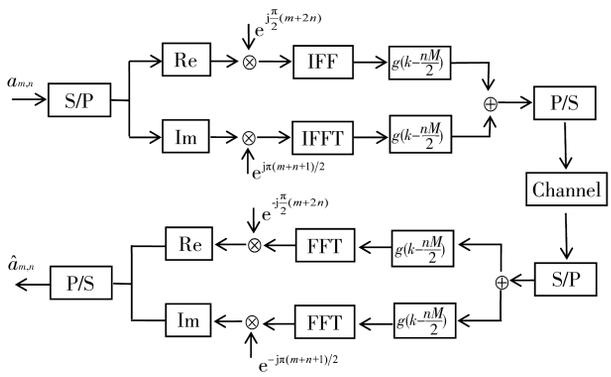

Fig. 1 FBMC/OQAM system block diagram

According to the system model, the baseband transmission signal $s(k)$ of the FBMC/OQAM system can be expressed as

$$s(k)=\sum_{m=0}^{M-1}\sum_{n\in\mathbf{Z}}a_{m,n}g\left(k-\frac{nM}{2}\right)e^{\frac{j2\pi mk}{T}}e^{j\frac{(m+n)\pi}{2}}, \quad (1)$$

where the position of $a_{m,n}$ is represented by a time frequency point (TFP) (m,n); $g_{m,n}(k)$ represents

the subcarrier basis function at (m, n), and the expression is

$$g_{m,n}(k) = g\left(k - \frac{nM}{2}\right) e^{\frac{j2\pi mk}{T}} e^{j\frac{(m+n)\pi}{2}}. \quad (2)$$

The demodulated symbol $\hat{a}_{m_0,n_0}$ at the ideal channel (m_0, n_0) is expressed as

$$\hat{a}_{m_0,n_0} = \sum_{k=0}^{\infty} s(k) g\left(k - \frac{nM}{2}\right) e^{\frac{-j2\pi mk}{T}} e^{-j\frac{(m+n)\pi}{2}} = \sum_{k=0}^{\infty} \sum_{m=0}^{M-1} \sum_{n\in\mathbf{Z}} a_{m,n} g\left(k - \frac{nM}{2}\right) e^{\frac{j2\pi mk}{T}} e^{j\frac{(m+n)\pi}{2}} \cdot g^*\left(k - \frac{nM}{2}\right) e^{\frac{-j2\pi mk}{T}} e^{-j\frac{(m+n)\pi}{2}} = \sum_{k=0}^{\infty} \sum_{m=0}^{M-1} \sum_{n\in\mathbf{Z}} a_{m,n} g_{m,n}(k) g^*_{m_0,n_0}(k). \quad (3)$$

According to the definition of the ambiguity function, the orthogonality condition of the FBMC/OQAM system can be expressed as

$$\xi_{m,n}^{m_0,n_0} = \sum_k g_{m,n}(k) g^*_{m_0,n_0}(k) = \sum_{m=0}^{M-1} \sum_{n\in\mathbf{Z}} g\left(k - \frac{nM}{2}\right) e^{\frac{j2\pi mk}{T}} e^{j\frac{(m+n)\pi}{2}} \cdot g^*\left(k - \frac{nM}{2}\right) e^{\frac{-j2\pi mk}{T}} e^{-j\frac{(m+n)\pi}{2}}, \quad (4)$$

where $\xi_{m,n}^{m_0,n_0}$ is 1 when $(m,n)=(m_0,n_0)$, and when $(m,n)\neq(m_0,n_0)$, the interference term between the filters is expressed as a pure imaginary number in the frequency domain[15]. Therefore, $\hat{a}_{m_0,n_0}$ in Eq. (3) can be expressed as

$$\hat{a}_{m_0,n_0} = a_{m_0,n_0} + \sum_{m=0}^{M-1} \sum_{n\in\mathbf{Z}} a_{m_0,n_0} \xi_{m,n}^{m_0,n_0} = a_{m_0,n_0} + ja^*_{m_0,n_0}. \quad (5)$$

It can be seen from Eq. (5) that if you want to recover the original signal, you need to perform the real part operation to eliminate the imaginary part interference.

1.2 Temperature and underwater acoustic communication

Changes in the marine environment will affect the performance of underwater acoustic communications. This section examines the impact of changes in water temperature on communications. The transmission of sound in the ocean will be affected by the physical and chemical properties of seawater and the sound will travel the sea through many paths. The specific path of propagation depends on the sound velocity structure in the water and the location of the transmitter and receiver[14]. Sound speed c is a function of temperature T, depth z (or pressure) and seawater salinity S[16]. The speed of sound (units of m/s) in a shallow water channel can be expressed as

$$c = 1\,412 + 3.21T + 1.19S + 0.016\,7z. \quad (6)$$

Transmission loss (L_{tr}) is defined as the cumulative decrease in sound intensity when sound waves propagate outward from the source. The acoustic signal in shallow water propagates within a cylinder bounded by a surface of water and seabed, forming a cylindrical diffusion. The transmission loss caused by cylindrical diffusion and absorption can be expressed as

$$L_{tr} = 10\log r + \alpha r \times 10^{-3}, \quad (7)$$

where α is the absorption coefficient (dB/km) and r is transmission distance (m). Due to the presence of trace amounts of boric acid ($B/(OH)_3$) and magnesium sulfate ($MgSO_4$) in the ocean, the transmission of sound waves in the ocean is mainly attenuated by viscous absorption (viscosity can be considered as the flow resistance of the fluid) and ion relaxation effects[17]. The expression of the absorption coefficient α is[1,18-19]

$$\alpha = \frac{A_1 P_1 f_1 f^2}{f^2 + f_1^2} + \frac{A_2 P_2 f_2 f^2}{f^2 + f_2^2} + A_3 P_3 f^2, \quad (8)$$

where f_1 represents the relaxation frequency of $B/(OH)_3$, kHz, and the expression is

$$f_1 = 2.8\left(\frac{S}{35}\right)^{0.5} \times 10^{[4-1\,245/(273+T)]}, \quad (9)$$

where S is salinity, 1/1 000; T is temperature, ℃; f_2 represents the relaxation frequency of $MgSO_4$, kHz, and the expression is

$$f_2 = \frac{8.17 \times 10^{[8-1\,990/(273+T)]}}{1 + 0.001\,8(S-35)}; \quad (10)$$

A_1 represents the $B/(OH)_3$ component in seawater and it can be expressed as

$$A_1 = \frac{8.68}{c} 10^{(0.78PH-5)}, \quad (11)$$

where PH represents the PH of water and c is the speed of sound; P_1 represents the depth pressure to which the $B/(OH)_3$ component in seawater is subjected, and it can be expressed as

$$P_1 = 1; \quad (12)$$

A_2 represents the $MgSO_4$ component in seawater and it can be expressed as

$$A_2 = 21.44\frac{S}{c}(1+0.025T); \quad (13)$$

P_2 represents the depth pressure of $MgSO_4$ component in seawater and it can be expressed as

$$P_2 = 1-1.37\times10^{-4}z+6.2\times10^{-9}z^2; \quad (14)$$

A_3 represents the pure water (viscosity) component in seawater, and its expression is

$$A_3=\begin{cases}4.937\times10^{-4}-2.59\times10^{-5}T+\\ 9.11\times10^{-7}T^2+9.11\times10^{-7}T^2-\\ 1.50\times10^{-8}T^3, & T\leqslant 20\ ℃,\\ 3.964\times10^{-4}+1.146\times10^{-5}T+\\ 1.45\times10^{-7}T^2-6.5\times10^{-10}T^3, & T>20\ ℃;\end{cases} \quad (15)$$

and P_3 indicates the pressure to which the pure water (viscosity) component is subjected,

$$P_3 = 1-3.83\times10^{-5}z+4.9\times10^{-10}z^2. \quad (16)$$

The traditional absorption coefficient model is only a function of frequency, such as the Thorp model. The absorption coefficient model used in this paper includes environmental factors such as temperature, salinity, pH value and water depth. Due to this paper studies the relationship between temperature factor and underwater acoustic communication, other underwater environmental factors are limited: salinity is set to the global observation average of 35 ppt, depth is 20 m, $PH=8$, and the absorption coefficient can be expressed as $\alpha(T,f)$. Then the transmission loss in the shallow water area is expressed as

$$L_{tr}(r,T,f) = 10\log r+\alpha(T,f)r\times10^{-3}. \quad (17)$$

The sound velocity curve and absorption coefficient will be affected by temperature changes, which will actually change transmission loss and BER. In the research of underwater acoustic channel estimation technology, the emphasis is on reducing the BER and improving the performance of underwater acoustic communication.

2 Pilot-based underwater acoustic channel estimation technique for FBMC/OQAM systems

2.1 Traditional interference approximate channel estimation algorithm

Suppose the channel of each subcarrier is a flat channel, $\eta(k)$ is an additive white Gaussian noise with a mean of zero, so the received signal can be expressed as

$$y(k) = \sum_{m=0}^{M-1}\sum_{n\in\mathbf{Z}}a_{m,n}g_{m,n}(k)H_{m,n}+\eta(k), \quad (18)$$

where $H_{m,n}$ represents the channel impulse response in the frequency domain. The received $\hat{a}_{m_0,n_0}$ is demodulation of the n_0-th FBMC/OQAM symbol on the m_0-th subcarrier, which can be expressed as

$$\hat{a}_{m_0,n_0} = H_{m_0,n_0}a_{m_0,n_0}+\sum_{(m,n)\neq(m_0,n_0)}H_{m,n}a_{m,n}\xi_{m,n}^{m_0,n_0}+\eta_{m_0,n_0} = H_{m_0,n_0}a_{m_0,n_0}+\sum_{(p,q)\neq(0,0)}H_{m_0+p,n_0+q}a_{m_0+p,n_0+q}\xi_{m_0+p,n_0+q}^{m_0,n_0}+\eta_{m_0,n_0},\ (m=m_0+p,\ n=n_0+q). \quad (19)$$

According to Eq. (4), when $(m,n)\neq(m_0,n_0)$, $\xi_{m,n}^{m_0,n_0}$ is a pure imaginary value, so $\hat{a}_{m_0,n_0}$ can be further expressed as

$$\hat{a}_{m_0,n_0} = H_{m_0,n_0}(a_{m_0,n_0}+ja_{m_0,n_0}^*)+\eta_{m_0,n_0}. \quad (20)$$

Suppose that the pilot symbol is inserted at (m_0, n_0), $u_{m_0,n_0} = ja_{m_0,n_0}^*$ is the imaginary interference caused by (m_0,n_0) first-order neighborhood Ω_{m_0,n_0}.

$$c_{m_0,n_0} = a_{m_0,n_0}+u_{m_0,n_0} = a_{m_0,n_0}+ja_{m_0,n_0}^*, \quad (21)$$

where c_{m_0,n_0} is the equivalent pilot data transmitted at the time-frequency grid point (m_0, n_0). When the transmitted pilot symbol a_{m_0,n_0} and the neighbor range Ω_{m_0,n_0} are known, the channel frequency domain response is estimated at (m_0,n_0),

$$\hat{H}_{m_0,n_0} = \frac{\hat{a}_{m_0,n_0}}{c_{m_0,n_0}} = H_{m_0,n_0}+\frac{\eta_{m_0,n_0}}{a_{m_0,n_0}+ja_{m_0,n_0}^*}. \quad (22)$$

It can be seen from Eq. (22) that if the accuracy of the channel estimation value is improved, the second term of the interference term on the right side of Eq. (22) is operated to minimize the interference of the channel estimation.

2.2 Improved IAM pilot channel estimation

From the above analysis, the interference term is the product of the symbols around the pilot and the internal product of the subcarrier basis function corresponding to the TFP. And the inner product of the prototype filter function called as the time-frequency offset is the interference coefficient[13]. The interference weight coefficient matrix is generally expressed as

$$\boldsymbol{W} = \begin{bmatrix}(-1)^{m_0}\delta & -\beta & (-1)^{m_0}\delta\\ -(-1)^{m_0}\gamma & 1 & (-1)^{m_0}\gamma\\ (-1)^{m_0}\delta & \beta & (-1)^{m_0}\delta\end{bmatrix}. \quad (23)$$

The expression of interference weight coefficient is shown in Eq. (24). This paper takes $\beta=0.323\ 9$, $\gamma=0.566\ 4$, $\delta=0.205\ 8$.

$$\begin{cases}\beta=\sum_k g^2(k)\mathrm{e}^{\mathrm{j}(2\pi/M)k},\\ \gamma=\sum_k g(k)g(k-M/2),\\ \delta=-\mathrm{j}\sum_k g(k)g(k-M/2)\mathrm{e}^{\mathrm{j}(2\pi/M)k}.\end{cases}\tag{24}$$

The transmission loss L_{tr} in underwater acoustic communication has been obtained in the previous section. When the distance and frequency of the receiving end are fixed, the power of the received signal P_{r} is

$$P_{\mathrm{r}}=\frac{P_{\mathrm{t}}}{L_{\mathrm{tr}}(T)},\tag{25}$$

where P_{t} represents the power of the transmitted signal. The core principle of IAM channel estimation is to increase the equivalent pilot power and reduce the impact of noise on channel estimation. Guided by the idea of maximizing the equivalent pilot power, let a_1 be the amplitude of the pilot in an ideal environment, then the amplitude of the pilot in underwater acoustic communication can be expressed as

$$a=\sqrt{\frac{a_1^2}{L_{\mathrm{tr}}(T)}}=\frac{1}{L_{\mathrm{tr}}(T)}a_1.\tag{26}$$

Assuming that the transmission signal power is constant, the smaller the transmission loss caused by temperature, the better the effect of IAM channel estimation. Therefore, this paper proposes a new pilot structure to improve the impact of transmission loss on channel estimation.

2.2.1 New IAM pilot structure design

In the past channel estimation studies based on the FBMC system, the channels used were all maritime wireless channels. In this paper, the FBMC/OQAM channel estimation method with different pilot structure is simulated in the underwater acoustic channel. It is found that the channel estimation performance by introducing complex structure pilot sequences is better than the traditional IAM-C and EIAM-C schemes. The pilot structure is designed according to Eqs. (23)—(24).

In the pilot structure shown in Fig. 2, when the subcarrier $m\leqslant 3$, the pilot data is 0. When the subcarrier $m\in\{4,5,\cdots,M-1\}$ is in the middle position, take the pilot sequence [1−j j −1+j −j] as a cyclic sequence, and according to the value of the intermediate pilot sequence, discuss the power of the equivalent pilot data in the structure. When the intermediate pilot data is $\pm1\mp\mathrm{j}$, the number of subcarriers is odd, and the pilot sequence values on both sides are 0. At this time, the pilots of the left and right columns have an equivalent pilot power, that is $P_1=a^2|-1+\mathrm{j}+2\beta|^2=3.186\ 3a^2$. It is worth noting that at $m=5$, the equivalent pilot power is $3.088\ 3a^2$, which is approximately equal to P_1. When the subcarrier is in the even position, the intermediate pilot sequence is $\pm\mathrm{j}$, the pilot sequences on both sides are placed at $\mp\mathrm{j}$, the equivalent pilot power is $P_2=a^2|1+2\beta-2\mathrm{j}\beta|^2=2.415\ 3a^2$. Different from the EIAM-C pilot structure, the proposed pilot data of the left and right sides of the new IAM pilot structure are the same, so the interference weight coefficient γ does not contribute to the equivalent pilot power. The new IAM pilot structure has an equivalent pilot power of $P=(P_1+P_2)/2=2.800\ 7a^2$. By comparison analysis, the equivalent pilot power fluctuates between IAM-C and EIAM-C.

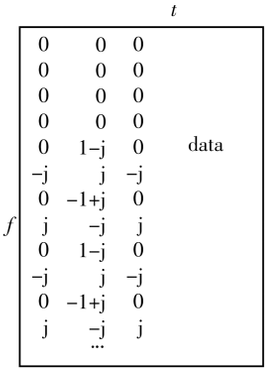

Fig. 2 New IAM pilot structure

2.2.2 Iterative based IAM pilot channel estimation

In order to further improve the estimation accuracy, the IAM pilot structure proposed in this paper is iteratively operated, and the estimation error is reduced by reconstructing the equivalent pilot. The steps are as follows:

Step 1: Demodulate the pilot symbols received at the receiver to obtain an equivalent pilot;

Step 2: Based on the obtained equivalent pilot c_{m_0,n_0}, obtain the channel estimate $\hat{H}$ at the time-frequency grid point.

Step 3: Using the estimated value $\hat{H}$ obtained by Step2 and the data demodulated by the time-frequency grid point, the equivalent pilot is reconstructed according to Eq. (20) to obtain c'_{m_0,n_0}.

Step 4: The interference amount of the equivalent pilot to the channel estimation value obtained by

Eq. (22) is subtracted from the interference amount by the $\hat{H}$ calculated by Step 2 to obtain a more accurate channel estimation value $\hat{H}'$.

Step 5: Set the number of iterations in advance and repeat Step 3 and Step 4 to get a more accurate channel estimate.

3 Simulation experiment

This section selects the underwater acoustic channel environment and verifies the performance of the algorithm through Matlab simulation. The parameter settings are shown in Table 1. The characteristics of underwater acoustic channel include bandwidth limitation, multipath effect, Doppler effect, ocean environment noise and time variation of channel. Fig. 3 is the shallow seawater acoustic channel impulse response diagram selected in this paper.

Table 1 Simulation parameters

Parameter	Value
Number of subcarriers	128
FBMC number of symbols	10
Modulation	QAM
Prototype filter	PHYDYAS
Overlap factor	4
Sampling rate (Hz)	128
Number of simulations	10

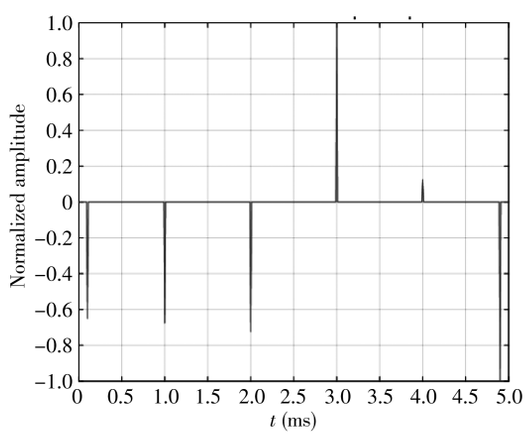

Fig. 3 Shallow seawater acoustic channel impulse response diagrame

The iterative channel estimation method(It-IAM) based on the new pilot structure proposed in this paper and the channel estimation method based on the traditional IAM-C and EIAM-C pilot structure are simulated. Fig. 4 is a comparison diagram of BER of different pilot channel estimation methods in the above-described underwater acoustic channel environment. In Fig. 4, the channel estimation of It-IAM with the iteration of 0, 1 time and 2 times are compared. It can be seen that the performance of estimation is average when there is no iteration, the performance is significantly improved after 1 time iteration, and when the iteration is 2 times, the performance is not significantly improved compared to the 1 time iteration. Since the equivalent pilot power of the It-IAM pilot structure fluctuates between the equivalent pilot power values of IAM-C and EIAM-C, when the It-IAM channel estimation is iterated 0 time, the BER curve is also located in the middle. It can be seen from Fig. 4 that the channel estimation after 1—2 iterations has an improvement of about 3—4 dB over EIAM-C at a BER of 10^{-2}.

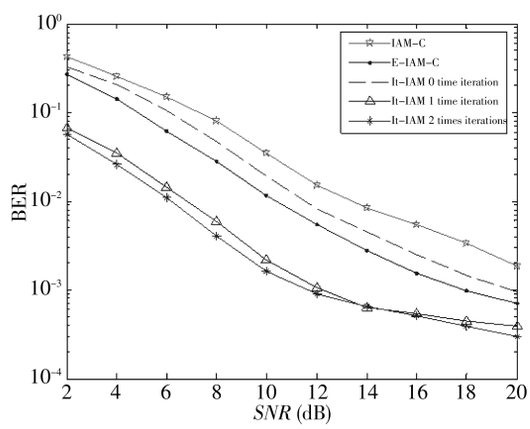

Fig. 4 Performance comparison of algorithms in underwater acoustic channel (1)

In order to verify the effect of the algorithm proposed in this paper on underwater acoustic communication channels, there is a comparison and verification of pilot channel estimation methods based on IAM. Fig. 5 shows the simulation of IAM-R, IAM-I, IAM-C, EIAM-C and It-IAM with iterating 1 time. From this similation, it can be seen that in the same underwater environment, It-IAM algorithm proposed in this paper has the best performance.

In the second section, the influence of temperature on the underwater acoustic communication process is analyzed. According to Eqs. (8)—(16), the relationship between seawater absorption coefficient and underwater temperature can be obtained, as shown in Fig. 6. From Eq. (7), it can be found that the transmission loss is positively correlated, so the relationship between transmission loss and temperature in the underwater acoustic communication process can also be represented by the curve shown in Fig. 6. The It-IAM channel estimation performance introduced in this paper gradually increases with temperature increase when it is lower than 8 ℃, and the performance is negatively

correlated when the underwater temperature exceeds 8 ℃.

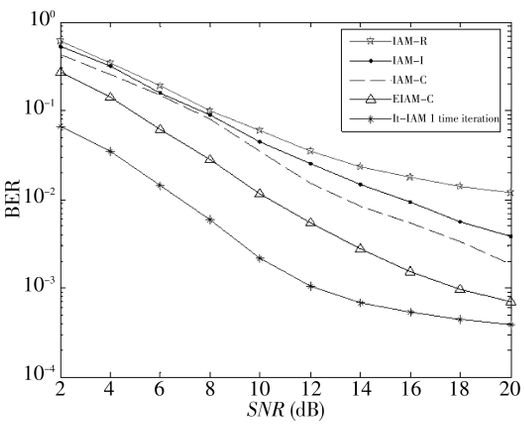

Fig. 5 Performance comparison of algorithms in underwater acoustic channel (2)

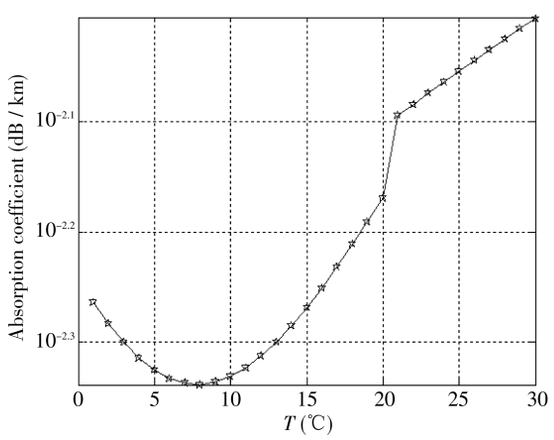

Fig. 6 Underwater absorption coefficient and temperature diagram

4 Conclusion

The paper applied the FBMC/OQAM system to the underwater, the influence relationship between temperature factors and underwater acoustic communication was analyzed comprehensively. By studying the FBMC/OQAM channel estimation technique, an iterative channel estimation method for new pilot structure was proposed. It-IAM increased the equivalent pilot power by introducing complex numbers in the pilot structure design, and also reduced the interference of noise on channel estimation, and inserted zero value at the front end of the pilot structure in response to the frequency shift and delay characteristics of the underwater acoustic channel. The algorithm performance is verified by simulation experiments, and the influence of underwater acoustic channel with different temperature on channel estimation performance is summarized. In the future, the underwater acoustic channel estimation technology will be studied in combination with the underwater salinity and depth factors to improve the underwater performance of the FBMC/OQAM communication system.

References

[1] Schellmann M, Zhao Z, Lin H, et al. FBMC-based air interface for 5G mobile: challenges and proposed solution. In: Proceedings of 9th International Conference on Cognitive Radio Oriented Wireless Networks and Communications(CROWNCOM), IEEE, 2014: 102-107.

[2] Eiayoubi S E, Boldi M, Bulakci O, et al. Preliminary views and initial considerations on 5G RAN architecture and functional design. Project White Paper METIS II, 2016: 1-27.

[3] Viholainen A, Bellanger M, Huchard M. Phydas-physical layer for dynamic access and cognitive radio. Report, 2009, (5): 1.

[4] Du J, Signell S. Time frequency localization of pulse shaping filters in OFDM/OQAM systems. In: Proceedings of 6th International Conference on Information, Communications & Signal Processing, IEEE, 2007: 1-5.

[5] Gharba M, Legouable R, Siohan P. An alternative multiple access scheme for the uplink 3GPP/LTE based on OFDM/OQAM. In: Proceedings of 7th International Symposium on Wireless Communication Systems, IEEE, 2010: 941-945.

[6] Wang C L, Wang S C. A new preamble design for channel estimation in offset QAM filter bank multicarrier systems. In: Proceedings of IEEE Global Communications Conference (GLOBECOM), IEEE, 2018: 1-6.

[7] Lélé C, Legouable R, Siohan P. Channel estimation with scattered pilots in OFDM/OQAM. In: Proceedings of IEEE 9th Workshop on Signal Processing Advances in Wireless Communications, IEEE, 2008: 286-290.

[8] Ni S X. Research on PAPR suppression and channel estimation technology of FBMC system. Hangzhou: Zhejiang University, 2019.

[9] He Z M, Zhou L Y, Yang Y, et al. DFT-based channel estimation refinement by clustering in FBMC-OQAM system. The Journal of Engineering, 2019, (3): 652-656.

[10] Lélé C, Javaudin J, Legouable R, et al. Channel estimation methods for preamble-based OFDM/OQAM modulations. European Transactions on Telecommunications, 2010, 19(7): 741-750.

[11] Du J, Signell S. Novel preamble-based channel estimation for OFDM/OQAM systems. In: Proceedings of IEEE International Conference on Communications, IEEE, 2009, 7(9): 4135-4140.

[12] Kofidis E, Katselis D. Improved interference approximation method for preamble-based channel estimation in FBMC/OQAM. In: Proceedings of Signal Processing Conference, IEEE, 2011, 10(19): 1603-1607.

[13] Fuhrwerk M, Moghaddamnia S, Peissig J. Scattered pi-

lot-based channel estimation for channel adaptive FBMC-OQAM systems. IEEE Transactions on Wireless Communications, 2017, 16(3): 1687-1702.
[14] Domingo M C. Overview of channel models for underwater wireless communication networks. Physical Communication, 2008, 1(3): 163-182.
[15] Liu G H, Li P. IAM preamble channel estimation algorithm based on iterative FBMC/OQAM system. Computer Measurement and Control, 2018, (10): 40.
[16] Geoffroy M, Daase M, Cusa M, et al. Mesopelagic sound scattering layers of the high arctic: seasonal variations in biomass, species assemblage, and trophic relationships. Frontiers in Marine Science, 2019, 6: 1-18.
[17] Kyhn L A, Waisniewska D M, Beedholm K, et al. Basin-wide contributions to the underwater soundscape by multiple seismic surveys with implications for marine mammals in Baffin Bay, Greenland. Marine Pollution Bulletin, 2019, 138: 474-490.
[18] Cottet E, Murphy P, Bassett C, et al. Acoustic characterization of sensors used for marine environmental monitoring. Marine Pollution Bulletin, 2019, 144: 205-215.
[19] Hildebrand J A, Frasier K E, Banmann P S, et al. Assessing seasonality and density from passive acoustic monitoring of signals presumed to be from pygmy and dwarf sperm whales in the Gulf of Mexico. Frontiers in Marine Science, 2019, 6: 66.

基于 FBMC 的水声信道估计与温度因素的研究

郭银景[1,2], 刘　珍[1], 杨文健[1], 牛晨曦[1], 刘　辉[1]

(1. 山东科技大学 电子信息工程学院, 山东 青岛 266590;
2. 青岛智海牧洋科技有限公司, 山东 青岛 266590)

摘　要: 水下环境的复杂性对水声通信带来挑战, 不同温度、深度和盐度的海洋环境对通信性能的影响值得关注。本文对温度因素影响下的水声信道进行分析, 为进一步研究基于滤波器组多载波(FBMC)水声信道估计问题提供了参考。将 FBMC/OQAM 调制技术引入水下, 研究基于 FBMC 的水声信道估计技术。通过改进导频结构来适应复杂多变的水声信道, 采用迭代方法获得精确度更高的信道信息, 进一步提高信道估计性能。理论分析和仿真结果表明, 本中所提的新基于干扰近似方法(IAM)导频迭代信道估计算法在水声信道中有更好的性能。

关键词: 滤波器组多载波(FBMC); 水声信道估计; 温度; 导频; 干扰近似方法(IAM)

引用格式: GUO Yin-jing, LIU Zhen, YANG Wen-jian, et al. Research on underwater acoustic channel estimation and temperature factors based on FBMC. Journal of Measurement Science and Instrumentation, 2020, 11(2): 197-204. [doi: 10.3969/j.issn.1674-8042.2020.02.013]